JOURNAL OF OPTOELECTRONICS AND ADVANCED MATERIALS Vol. 10, No. 8, August 2008, p. 1899 - 1903

Simulation code for the D^- beam transport through the ITER neutralizer

T. MINEA*, A. LIFSCHITZ, G. MAYNARD, K. KATSONIS, J. BRETAGNE, A. SIMONIN[a]
Laboratoire de Physique des Gaz et Plasmas – LPGP
Université Paris Sud XI, Bat. 210, 91405 Orsay Cedex, France
[a]DRFC, CEA Cadarache, 13108 Saint-Paul lez Durance, France

This paper reports the first results on the negative ions beam transport through the ITER neutralizer by the recently developed numerical tool OBI-2 (Orsay Beam Injector, two dimensional code) based on the Particle-in-Cell approach coupled with the Monte Carlo treatment of collisions. The choice of the elementary processes involved in the D^- / D_2 interaction are discussed as well as the related plasma/wall processes. The latter dominates over the interaction between particles composing the residual weakly ionized plasma. The formation of the residual plasma is demonstrated and its role on the beam transport is emphasized.

(Received March 1, 2008; accepted June 30, 2008)

Keywords: Additional heating in ITER, Negative ions, High energy neutral beam, Particle-in-Cell

1. Introduction

In the future experimental fusion reactor ITER, external heating sources are needed to compensate the Ohmic heating decrease when the plasma temperature increases, and to achieve self-sustained plasma conditions through fusion reactions [1]. Heating of plasma ions will be performed through the injection of energetic D° beams. The two Neutral Beam Injectors (NBI) designed for ITER should bring a power of about 35 MW. In order to reach the plasma core, externally injected D° atoms must have an energy of 1 MeV. Each NBI is composed by four parts: the negative ion source (40 A of D^-), the accelerator (1 MV single gap or multi-grid), the neutralizer (for the conversion of D^- in D°), and the ion deflector (for the removal of charged particles remaining in the beam at its exit from the neutralizer, ~20% D^- and ~20% D^+). The neutralizer is crucial for the final NBI performances, because the beam transport and conversion across it will determine ultimately the neutral beam properties just before entering the ITER vacuum chamber.

The present work was undertaken to evaluate the efficiency of the NBI in terms of negative ion beam conversion into neutrals and beam geometrical properties at extraction for several designs using the recently developed numerical tool OBI-2 (Orsay Beam Injector, two dimensional code). The ionization induced by the D^- beam on the buffer gas (D_2) filling the neutralizer creates a rarefied residual low-temperature plasma (ionisation degree ~ 10^{-3}, electron temperature < 20 eV). The role and dynamics of the residual plasma will also be treated. This plasma can screen the electrostatic well of the D^- beam and, consequently, affect the properties of the extracted beam emittance and the energy transport to the neutralizer walls. Some results are presented here. Further developments of the modeling are discussed.

2. Numerical simulation

The Particle-in-Cell code OBI-2, initially developed at LPGP for heavy ion inertial fusion [2,3], was upgraded to include the induced plasma by the beam propagation and the related secondary particle interactions by Monte Carlo collision (MCC) method. The geometry of the neutralizer used in the present work has been chosen as 2D cylindrical symmetry which is not the real configuration of the neutralizer plates, but remains realistic in terms of the volume to surface aspect ratio. This 2D(r,z) simplified geometry is more realistic than 1D treatment used in the analytical model [4]. Assuming an azimuthal symmetry of the problem, we get information not only along the beam axis (z), but also along the radial one (r). Therefore it is possible to follow the residual plasma formed between the symmetry axis and the wall. Simulations reported in this paper are electrostatic, 2 1/2 dimensional. For the sake of simplicity, the trajectories are followed in Cartesian coordinates and then projected to cylindrical coordinates (r,z,v_x,v_θ,v_z).

The code integrates the particle beam trajectories including volume processes and particle-wall interaction. OBI-2 follows the kinetics of stripped electrons which lead to the residual plasma development and includes an electrostatic solver for the determination of the 2D map of the electric field within the neutralizer.

We assume a negative ion beam (D^-) entering a copper grounded tube of 50 mm radius and 3000 mm

length. In the neutralizer, the D^- beam of 1 MeV interacts with D_2 gas. Consequently, negative ions are mainly converted to fast D° atoms. In addition, some negative ions can loose both electrons (double stripping) thus creating fast D^+ ions. The main processes involving the beam particles are the following:

electron detachment $D^- + D_2 \rightarrow D° + D_2 + e_s$ Refs. [5,6,7,8] (1)

double stripping $D^- + D_2 \rightarrow D^+ + D_2 + 2\,e_s$ Ref. [5] (2)

ionization of neutrals $D° + D_2 \rightarrow D^+ + D_2 + e_s$ Ref. [5] (3)

in which e_s represents stripped electrons which are assumed to follow the beam particle after the ionization. The charge exchange reaction between D^+ and D_2 has been neglected, the corresponding cross-section being very low at 1 MeV. In the present version of the code, a frozen D_2 buffer gas inside the neutralizer is assumed for the kinetic treatment of the electrons and heavy particles ($D°$, D^+, D^-, D_2^+).

Beam particles also produced ionization of the buffer gas through the following processes,

$D^+ + D_2 \rightarrow D^+ + D_2^+ + e$ Refs. [5,9,10] (4)

$D^0 + D_2 \rightarrow D^0 + D_2^+ + e$ Ref. [5] (5)

$D^- + D_2 \rightarrow D^- + D_2^+ + e$ (6)

Stripped electrons which are created at 272 eV by beam particles of 1 MeV as well as electrons resulting from D_2 ionization can also lead to further ionization

$e + D_2 \rightarrow e + D_2^+ + e$ Ref. [11] (7)

leading, at the end of the energy degradation process, to a low temperature plasma.

The cross section for the process given in reaction (6) is taken as the sum of the corresponding cross sections for the processes (5) and (7).

At the present stage of the code development the kinetics of plasma heavy particles is quite limited. We neglect processes such as electron impact dissociation and reactions between neutral and ionic atoms or molecules. Consequently, the secondary plasma consists of the products of the sole selected reactions, for instance the molecular ion D_2^+ is the positive species. Processes neglected for the moment have to be checked in terms of sensitivity in the future. However, this first version of the model permits to show the build-up of the residual plasma and its consequences of the particle beam transport.

The NBI geometry and the buffer gas density are such that collisions of beam particles with neutralizer wall do happen. Then, several phenomena can occur to the walls (neutralization, secondary electron emission, sputtering of the walls etc.). For the moment, only reflections at specular angle are considered for the beam particles and electron secondary emission on the walls by stripped electron impact. Note that collisions of the residual plasma species with the walls are dominant over gas phase collisions.

3. Results and discussion

Gas density presents an axial gradient since the target gas (D_2) is injected at the mid-plane of the neutralizer [12]. The simulation box starts from the extraction grid (z = 0 m in Figs. 1, 2, and 3) biased at -0.94 MV. The neutralizer entrance plane is located at z = 2 m and the exit plane at z = 5 m. The injected beam is composed of 1 MeV D^-. The results reported here have been obtained for two conditions of the beam diameter, while keeping constant its current density (~200 Am^{-2}). The first condition corresponds to a beam current is 0.031 A; its entrance radial profile is square with a radius of 6 mm.

Fig. 1 shows the density of each species of beam heavy particles, D^- (Fig. 1(a)), D^0 (Fig. 1(b)), and D^+(Fig. 1(c)) at t=24 μs. It can be seen that the beam radius is roughly constant along the neutralizer and this happens when the residual plasma develops (typically after 10 μs). Moreover, Fig. 1 represents the conversion of negative ions into fast neutrals and positive ions. As soon as the beam enter the neutralizer (z = 2 m), the first fast neutrals appear (blue colour - Fig. 1(b)), but the maximum (red colour - Fig. 1(b)) is found at the exit plane (z = 5 m) and on the beam axis. In contrast, positive ions appear further to the entry plane, close to the centre of the neutralizer (z ~3 m, Fig. 1(c)), and their density increases along the beam, reaching also a maximum at the exit plane. This is coherent with the ionization of fast neutrals which can be converted in positive ions (two step process). However, the double stripping process is much less efficient as source term for D^+ creation, and there is quite no effect when the beam crosses the first half path of the neutralizer (z < 3.5 m).

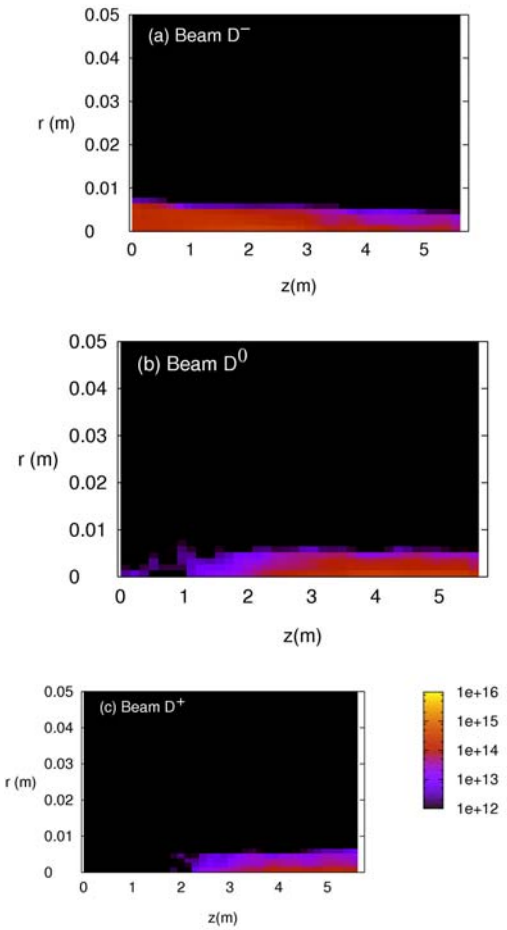

Fig. 1. Density of each type of heavy particle composing the beam of 2 cm in diameter at t = 24 µs, (a) D^- negative ions, (b) D° fast neutrals, (c) D^+ positive ions.

The heavy particle beam density (total density of D^-, D° and D^+) the electron beam density (electrons traveling with the beam) and the residual plasma densities, namely of electrons and D_2^+, are reported on Figure 2. In the radial direction, the stripped electron beam is very constricted with respect to the beam radius inside the neutralizer, but it diverges outside (z > 5 m; Fig. 2 (c)). That can be explained by their high mobility compared to heavy beam particles and their low transverse energy limited by the wall sheaths of the neutralizer. Outside, the sheath disappears and their radial expansion is not limited anymore. In the axial direction, the electrons composing the residual plasma have their density distribution shaped as the buffer gas one (Fig. 2(d)). In the radial direction, the wall sheath is well established after 10 µs. However, the plasma is very tenuous beyond the beam radius when approaching the walls. This indicates a loose correlation of the volume interactions with respect to the wall ones.

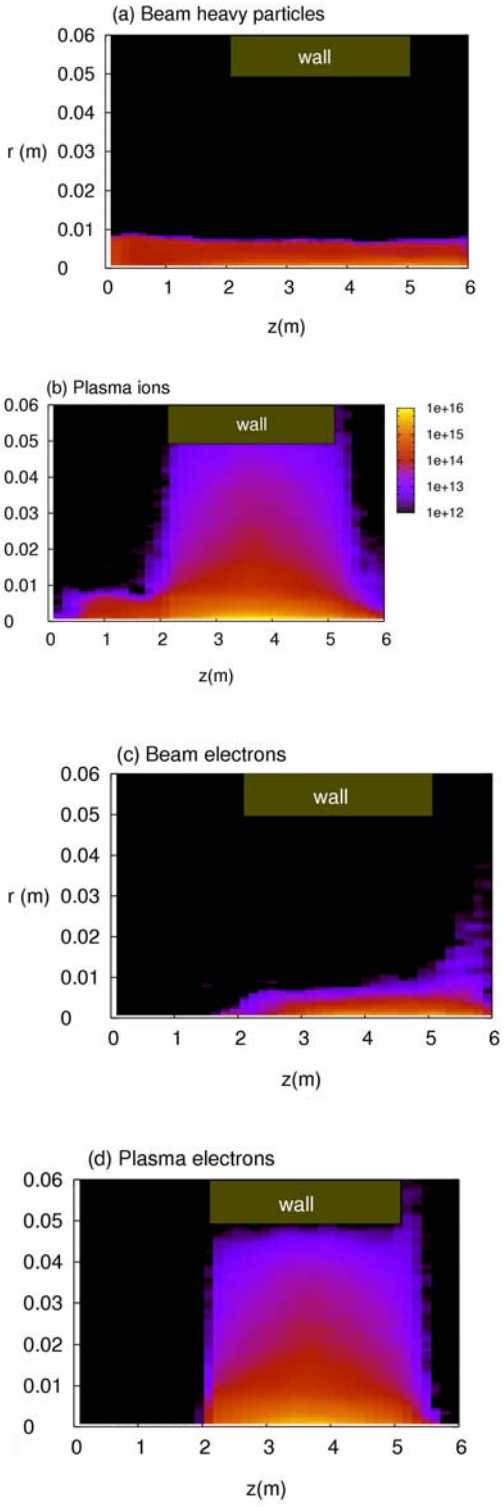

Fig. 2. Density distributions of a beam of 2 cm in diameter and of residual plasma particles at t = 24 µs, on logarithmic scale (m^{-3}). (a) beam heavy species (D^-; D°, D^+); (b) D_2^+ secondary plasma ions; (c) stripped electrons; (d) 'thermalized' plasma electrons.

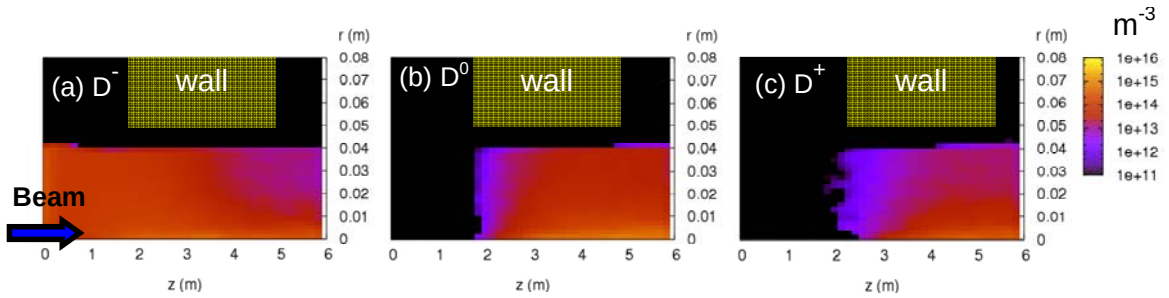

Fig. 3. Density of each type of heavy particle composing the beam of 8 cm in diameter at t = 10 µs, (a) D^- negative ions, (b) D° fast neutrals, (c) D^+ positive ions. The beam direction is indicated by the arrow.

The second condition corresponds to a beam current of 0.31 A with a larger beam of 80 mm diameter and square profile. Fig. 3 reports the density of D^- (Fig. 3(a)), D0 (Fig. 3(b)), and D+ (Fig. 3(c)) at t=10 µs. As for Fig. 1, the D^- beam density decreases and the D° beam density increases simultaneously, while the increase of the D^+ beam density is delayed with respect to the D° one.

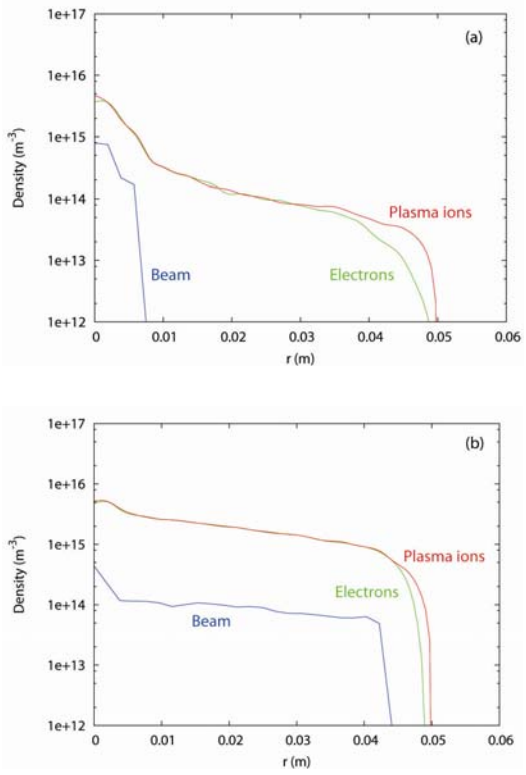

Fig. 4. Comparison of radial profiles of the density of plasma and beam particles at the mid-plane over a section of the neutralizer for (a) the small beam and (b) the larger one.

The radial distributions of beam and plasma species at the mid-plane of the neutralizer for the two beam dimensions are compared on Figure 4. In the two cases, stiff shoulders are observed for the beam ions profile. Significant differences are observed for residual plasma electrons and ions between the two conditions. The plasma neutrality, a relatively flat profile and a very narrow sheath near the walls are observed for the larger beam (40 mm radius, Fig. 4(b)). On the opposite, the quasi-neutrality is verified only for about 35 mm and plasma electron and ion profiles are more sloping for the small beam (6 mm radius, Fig. 4(a)). These differences can be explained by much higher plasma densities for the larger beam which is fed by two ionization sources, beam particles and secondary electron ionization.

It appears that for the reactions from (4) to (7) it is necessary to introduce the double differential cross section ($d\sigma/d\varepsilon d\theta$) where ε is the energy of the ejected electron and θ is the angle with respect to the projectile velocity. Our simulations suggest that the distributions of ε and θ for the ejected electron have a strong influence on the properties of the residual plasma (i.e. electron temperature, plasma density, …).

4. Concluding remarks

The novel numerical tool called OBI-2 is ready to work and it can be used for parametric investigations of the ITER neutralizer. OBI-2 was used to study two beam configurations for the ITER NBI, of 6 mm and of 40 mm radius, respectively. The beam kinetics seems analogous in both cases, while the residual plasma behaviour changes. For the small diameter beam, the density of the residual plasma drops beyond the beam radius. For the large beam, the residual plasma density is one order of magnitude larger, weakening slightly to the wall. In both cases the sheath is well established, quite large (~10 mm) for the small beam and much narrower (~3 mm) for the large one.

We have a first evidence of the role of the residual plasma in the confinement of the D^- negative ions inside the neutralizer. All heavy particles composing the beam are well collimated when leaving the neutralizer. Their

radial spread follows roughly the initial D^- beam diameter.

Further steps concerning the evolution of the present model are the introduction of double differential cross sections for gas phase collisions induced by the beam particles or by the residual plasma ones. The importance of the beam-wall interaction processes has to be checked together with their effect on the buffer gas heating and kinetics.

References

[1] D. R. Sweetman, Nuclear Fusion, **13**, 157 (1973)

[2] J.-L. Vay, C. Deutsch, in: E. Panarella (Ed.), Current Trends in International Fusion Research—Proceedings of the Third Symposium, Canada, 2002; J.-L. Vay, Ph. D. Thesis, Université Paris-Sud, Orsay (1996) (*in French*)

[3] A. Lifschitz, G. Maynard, J.-L. Vay, Nuclear Instruments and Methods in Physics Research A **544,** 202 (2005).

[4] E. Surrey, Nucl. Fusion, **46**, S360 (2006).

[5] IAEA AMDIS ALADDIN Database: www-amdis.iaea.org/ALADDIN/

[6] R. K. Janev, D. Reiter, U. Samm, "Collision Processes in Low-Temperature Hydrogen Plasmas", Rapport EIRENE: www.eirene.de/

[7] J. Geddes, J.Hill, M.B. Shah, T.V. Goffe, H. B. Gilbody, J. Phys. B **13**, 319 (1980).

[8] M. S. Huq, L.D. Doverspike, R.L. Champion, Phys. Rev A. **27,** 2831 (1983); J.S. Risley, R. Geballe, Phys. Rev. A **9**, 2485 (1974); G.I. Dimov, V.G. Dudnikov, Sov. Phys.-Tec.Phys. **11**, 919 (1967); A.C. Whittier, Can. J. Phys. **32**, 275 (1954).

[9] M.B. Shah, P.McCallion, and H.B. Gilbody, J. Phys. B, **22,** 3983 (1989); V.V. Afrosimov, G. A. Leiko, Yu A. Mamaev, and M. N. Panov, Sov. Phys. JETP **29**, 648 (1969); G.W. McClure, Phys. Rev. **148**, 47 (1966)

[10] M.B. Shah, H.B. Gilbody, J. Phys. B, **15,** 3441 (1982); S.B. Nesbitt, M.B. Shah, C.F.C. O'Rourke, C. McGrath, J. Geddes, D.S.F. Crothers, J. Phys. B, **33**, 637 (2000)

[11] T. Simko, PhD. Thesis, Université Paris-Sud, Orsay (1997) (*in French*)

[12] M. Dremel, EFDA - CCNB meeting, Culham, 22 to 24 May 2007.

*Corresponding author: tiberiu.minea@u-psud.fr